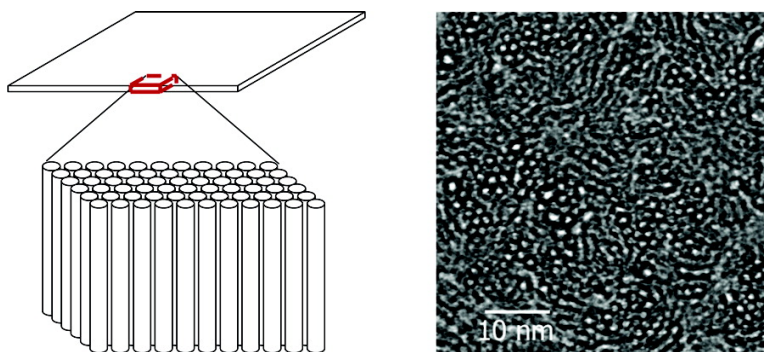


## Ultrathin “Bed-of-Nails” Membranes of Single-Wall Carbon Nanotubes

Yuhuang Wang, Sean Da, Myung Jong Kim, Kevin F. Kelly, Wenhua Guo, Carter Kittrell, Robert H. Hauge, and Richard E. Smalley

*J. Am. Chem. Soc.*, **2004**, 126 (31), 9502-9503 • DOI: 10.1021/ja048680j • Publication Date (Web): 16 July 2004

Downloaded from <http://pubs.acs.org> on April 1, 2009



### More About This Article

Additional resources and features associated with this article are available within the HTML version:

- Supporting Information
- Links to the 1 articles that cite this article, as of the time of this article download
- Access to high resolution figures
- Links to articles and content related to this article
- Copyright permission to reproduce figures and/or text from this article

[View the Full Text HTML](#)

## Ultrathin “Bed-of-Nails” Membranes of Single-Wall Carbon Nanotubes

Yuhuang Wang,<sup>†,‡</sup> Sean Da,<sup>§</sup> Myung Jong Kim,<sup>||</sup> Kevin F. Kelly,<sup>†,‡,#</sup> Wenhua Guo,<sup>○</sup> Carter Kittrell,<sup>†,‡</sup> Robert H. Hauge,<sup>†,‡</sup> and Richard E. Smalley<sup>\*,†,‡,||,○,#</sup>

Departments of Chemistry, Physics, and Electrical and Computer Engineering, Center for Nanoscale Science and Technology, Rice Quantum Institute, and Center for Biology and Engineering Nanotechnology, Rice University, MS-100, P.O. Box 1892, Houston, Texas 77251-1892, and FEI Company, 5350 NE Dawson Creek Drive, Hillsboro, Oregon 97124-5793

Received March 8, 2004; E-mail: smalley@rice.edu

Single-wall carbon nanotubes (SWNTs) are perfect 1-D objects with high aspect ratios and straight-through pores, whereby many of their extraordinary properties arise.<sup>1</sup> These objects, in principle, can be arranged in a membrane similar to a “bed-of-nails”, as shown in Figure 1a, in which a single layer of parallel SWNTs is densely packed and aligned along the normal to the membrane. Similar membranes made of carbon tubules with outside diameters as small as 9 nm have been previously synthesized.<sup>2</sup> The membranes display a range of interesting properties of technological importance, for example, electrochemical activities for reversible Li<sup>+</sup> intercalation,<sup>2a</sup> high capability for dispersion of platinum nanoparticles,<sup>2b</sup> and molecular transport across the membrane.<sup>2c</sup> Compared to the previous template-synthesized membranes, “bed-of-nails” membranes of SWNTs have two desirable properties: an ultrahigh pore density up to 10<sup>14</sup>/cm<sup>2</sup>, 2 to 3 orders higher than the previously reported carbon tubule membranes<sup>2</sup> and a narrow distribution of pore sizes that is tunable from ~0.4 to ~3 nm. Theoretical calculations<sup>3</sup> suggest that such a membrane combines both extremely high selectivity<sup>3a</sup> and flux<sup>3b</sup> toward molecule separations. Because of technical difficulties in either direct synthesis or postsynthesis processing, however, “bed-of-nails” membranes of SWNTs have not previously been demonstrated.

We have successfully created a proof-of-concept “bed-of-nails” SWNT membrane by milling a previously prepared<sup>4</sup> neat fiber of SWNTs with a gallium focused ion beam (FIB). Taking advantage of the preferential alignment of SWNTs along the fiber axis, we milled perpendicular to the fiber axis to produce a planar, free-standing, ultrathin, and single-walled carbon tubule membrane. The membrane can be as thin as 75 nm, allowing us to verify the special “bed-of-nails” arrangement with transmission electron microscopy (TEM). The surfaces of this membrane are almost completely free of amorphous carbon and Ga contamination, as confirmed by Raman spectra and energy-dispersive X-ray analysis (Supporting Information). Because of the special arrangement, the ends of the aligned SWNTs are readily accessible, enabling direct exploration of SWNT ends with various surface techniques. For example, with scanning tunneling microscopy (STM), we were able to determine the RMS surface roughness, which was as small as 0.6 nm in certain regions, and were able to further compare this surface to previously studied graphite and amorphous carbon surfaces.<sup>5</sup> We were able to cut through the whole fiber to reveal the cross section (Supporting Information), which provides critical information to our SWNT neat fiber spinning effort.<sup>4</sup> The approach is readily applicable to cutting

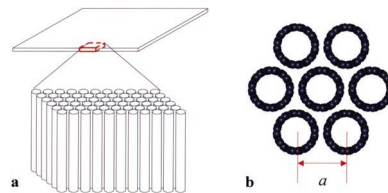


Figure 1. (a) Schematic of a “bed-of-nails” SWNT membrane. (b) SWNTs packed in a two-dimensional triangular lattice.

nanotubes to a desirable and precise length, which would otherwise end up with a broad distribution centered at a much longer length.<sup>6</sup> We believe this approach is extendable to other aligned nanotube materials (for example, nanotube membranes<sup>7a</sup> and as-grown strands<sup>7b</sup>) and, generally, to other carbon nanotube solid materials for site-specific internal structure analysis.

FIB milling was performed in a dual beam system (FEI Strata DB235) with “lift-out” techniques. The milling was performed by digital scan of the ion beam along the cutting direction.<sup>8</sup> The size of the TEM sample could be up to 15 μm × 15 μm with a thickness of 75 nm or less. Samples of larger area need to be thicker to avoid stress. Figure 2a shows a “bed-of-nails” SWNT membrane prior to being lifted out from the trench. The membrane can be placed across a hole in a holey TEM grid or on a marked position on a gold on mica substrate without causing any fracture. This technique may enable further fabrication of devices using the “bed-of-nails” membranes to test the transport properties of SWNTs.<sup>1,3,4</sup>

TEM observations were carried out in a JEOL JSM 2010 TEM operating at 100 kV accelerating voltage. Figure 2b is a bright field TEM image at low magnification from a corner of the membrane. The image appears darker where the electrons encounter more carbon atoms and are attenuated by scattering. Higher-magnification TEM images (Figure 2c,d) show a combination of dark lines and dark circles on a bright background. The dark lines are the images of tubule walls, while the dark circles appear where the axes of tube segments are approximately parallel to the electron beam. These dark circles generally exhibit brighter contrast than that observed from a curved SWNT rope. This is not surprising given that the tube axes are nearly parallel to the TEM electron beam. To maximize the population of the dark circles, the sample, which was generally off by a degree or two, was carefully tilted with a double tilt stage. Many dark circles were observed as clusters of 5–12 packed hexagonally. The dark circles were very sensitive to the tilt angle of the specimen. At a tilt of 0.1°, most dark circles would disappear while other circles in the vicinity might show up. At a tilt of 10° from the maximum population, almost no dark circles appeared, but short lines dominated (Figure 2d). Most of the lines appeared straight and had lengths of 10–16 nm as expected from

<sup>†</sup> Department of Chemistry, Rice University.

<sup>‡</sup> Center for Nanoscale Science and Technology, Rice University.

<sup>§</sup> FEI Company.

<sup>||</sup> Department of Physics, Rice University.

<sup>†</sup> Department of Electrical and Computer Engineering, Rice University.

<sup>#</sup> Rice Quantum Institute, Rice University.

<sup>○</sup> Center for Biology and Engineering Nanotechnology, Rice University.

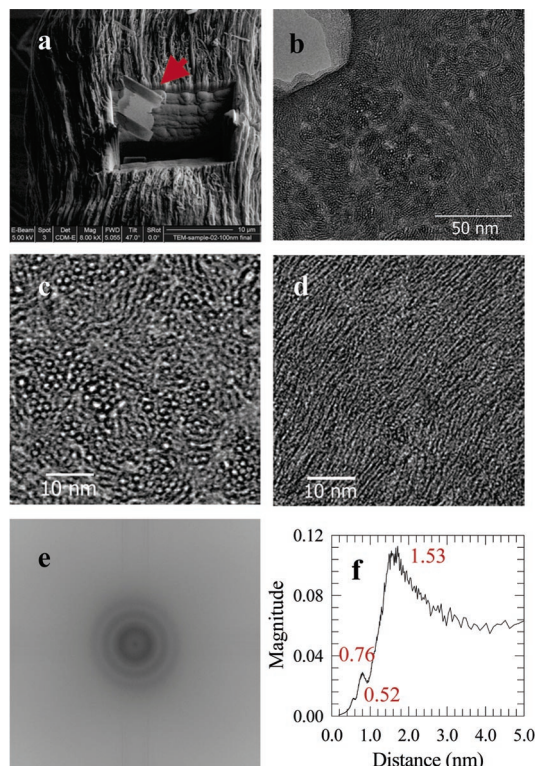


**Figure 2.** (a) A “bed-of-nails” SWNT membrane prior to lift out from the trench precreated in the side of a SWNT neat fiber (scale bar 10  $\mu\text{m}$ ). (b) Bright field image of a section of the membrane. (c) Magnified TEM image taken with electron beam approximately parallel to the normal of the membrane and (d) at 10° tilt. (e) Fourier transform of a typical TEM image. (f) Plot (e) as magnitude (circular average) vs distance.

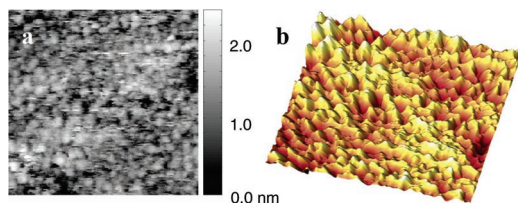


**Figure 3.** (a) STM topography,  $I = 0.1$  nA,  $V_{\text{sample}} = -0.5$  V,  $80 \times 80$  nm<sup>2</sup> scan area. (b) A 3-D image of the same topography.

straight SWNT segments of 75 nm long at the projection of 8–12°. Further observations indicated that nearly the entire membrane was uniform.

Figure 2e is Fourier transform of a typical TEM image (Supporting Information Figure 2a). Three isotropic rings are equally spaced. The circular average of these rings plotted in the real space shows three distinct peaks at 1.53, 0.76, and 0.52 nm, which, respectively, correspond to the lattice constant  $a$  of a hexagonal packing of SWNTs,  $a/2$ , and  $a/3$ , as expected. Given the van der Waals spacing,  $d_{vdw}$  (0.34 nm), of SWNTs in a rope,<sup>9</sup> we further derived that the distribution of nanotube diameters in our sample is peaked at 1.19 nm. This number is considerably larger than our earlier estimation from fluorescence measurement where only semiconducting tubes can be sampled.<sup>10</sup>

The “bed-of-nails” membrane was further investigated by ultra-high vacuum STM. The special “bed-of-nails” configuration made the SWNT ends readily accessible from the same surface. Figure 3 shows a representative STM topography of a “bed-of-nails” membrane dropped onto an atomically flat gold on mica substrate. The ends of the tubes appear 2–5 nm in diameter in the STM

images. While this is larger than the diameter of individual SWNTs measured by TEM, the discrepancy can be attributed to convolution with the finite size of the STM tip. This is common with STM images of similar objects. For instance, isolated C<sub>60</sub> with a van der Waals radii of 10.18 Å including the delocalized  $\pi$ -electrons typically appears with a diameter of 2 nm when imaged by STM.<sup>5a,b</sup> The measured RMS surface roughness varied somewhat depending on the size of the scan but was typically  $0.6 \pm 0.1$  nm over a 100 nm  $\times$  100 nm image. The STM images of these surfaces appear very different from those of graphite,<sup>5c</sup> amorphous carbon,<sup>5d</sup> or other amorphous surfaces.<sup>5e</sup>

It is not conclusive from this study whether the ends of the SWNTs in the “bed-of-nails” membranes are opened. However, it will not be surprising if the SWNTs are opened during the FIB milling process since the typical length of these tubes is 75 nm, which is over 15 times shorter than the average length of individual SWNTs in the fiber. In any case, both surfaces of the membranes are exposed, allowing further treatment with existing methods to open the ends.<sup>11</sup>

**Acknowledgment.** We gratefully thank Ramesh Sivarajan and Lars Ericson for the SWNT neat fiber. This work was supported by U.S. Department of Energy, the National Aeronautics and Space Administration, and Office of Naval Research.

**Supporting Information Available:** SEM images of the sidewall and cross section of SWNT neat fiber. Raman, additional TEM, and STM images of the “bed-of-nails” membranes. This material is available free of charge via the Internet at <http://pubs.acs.org>.

## References

- (1) Baughman, R. H.; Zakhidov, A. A.; de Heer, W. A. *Science* **2002**, *297*, 787.
- (2) For example: (a) Che, G.; Lakshmi, B. B.; Fisher, E. R.; Martin, C. R. *Nature* **1998**, *393*, 346. (b) Joo, S. H.; Choi, S. J.; Oh, I.; Kwak, J.; Liu, Z.; Terasaki, O.; Ryoo, R. *Nature* **2001**, *412*, 169. (c) Hinds, B. J.; Chopra, N.; Rantell, T.; Andrews, R.; Gavalas, V.; Bachas, L. *Science* **2004**, *303*, 62.
- (3) (a) Wang, Q.; Challa, S. R.; Sholl, D. S.; Johnson, J. K. *Phys. Rev. Lett.* **1999**, *82*, 956. (b) Skoulidas, A. I.; Ackerman, D. M.; Johnson, J. K.; Sholl, D. S. *Phys. Rev. Lett.* **2002**, *89*, 185901.
- (4) The fiber (HPR93B) was extruded from a 6 wt % SWNT/H<sub>2</sub>SO<sub>4</sub> dope through a 125- $\mu\text{m}$  orifice. For details, see: Zhou, W.; Vavro, J.; Guthy, C.; Winey, K. I.; Fischer, J. E.; Ericson, L. M.; Ramesh, S.; Saini, R.; Davis, V. A.; Kittrell, C.; Pasquali, M.; Hauge, R. H.; Smalley, R. E. *J. Appl. Phys.* **2004**, *95*, 649.
- (5) (a) Cuberes, M. T.; Schlittler, R. R.; Gimzewski, J. K. *Appl. Phys. Lett.* **1996**, *69*, 3016. (b) Lu, X.; Grobis, M.; Khoo, K. H.; Louie, S. G.; Crommie, M. F. *Phys. Rev. Lett.* **2003**, *90*, 096802/1. (c) Kelly, K. F.; Mickelson, E. T.; Hauge, R. H.; Margrave, J. L.; Halas, N. J. *Proc. Natl. Acad. Sci. U.S.A.* **2000**, *97*, 10318. (d) Schelz, S.; Richmond, T.; Kania, P.; Oelhafen, P.; Guentherodt, H. J. *Surf. Sci.* **1996**, *359*, 227. (e) Burgler, D. E.; Schmidt, C. M.; Schaller, D. M.; Meisinger, F.; Schaub, T. M.; Baratoff, A.; Guntherodt, H. J. *Phys. Rev. B* **1999**, *59*, 10895.
- (6) For example: (a) Liu, J.; Rinzler, A. G.; Dai, H. J.; Hafner, J. H.; Bradley, R. K.; Boul, P. J.; Lu, A.; Iverson, T.; Shelimov, K.; Huffman, C. B.; Rodriguezmacias, F.; Shon, Y. S.; Lee, T. R.; Colbert, D. T.; Smalley, R. E. *Science* **1998**, *280*, 1253. (b) Gu, Z.; Peng, H.; Hauge, R. H.; Smalley, R. E.; Margrave, J. L. *Nano Lett.* **2002**, *2*, 1009. (c) Lustig, S. R.; Boyes, E. D.; French, R. H.; Gierke, T. D.; Harmer, M. A.; Hietpas, P. B.; Jagota, A.; McLean, R. S.; Mitchell, G. P.; Onoa, G. B.; Sams, K. D. *Nano Lett.* **2003**, *3*, 1007.
- (7) For example: (a) Walters, D. A.; Casavant, M. J.; Qin, X. C.; Huffman, C. B.; Poul, P. J.; Ericson, L. M.; Haroz, E. H.; O’Connell, M. J.; Smith, K.; Colbert, D. T.; Smalley, R. E. *Chem. Phys. Lett.* **2001**, *338*, 14. (b) Zhu, H. W.; Xu, C. L.; Wu, D. H.; Wei, B. Q.; Vajtai, R.; Ajayan, P. M. *Science* **2002**, *296*, 884.
- (8) A Ga FIB (30 kV, 5 nA) was used for rough cut, (30 kV, 3 nA, and 1 nA) for the intermediate cut, which created a rectangular trench from both surfaces of the membrane, followed by a final polish with (10 kV, 100 pA, beam size 20 nm) to remove about 12 nm of amorphous carbon from each FIB cutting face.
- (9) Gao, G.; Cagin, T.; Goddard, W. A., III. *Nanotechnology* **1998**, *9*, 184.
- (10) Bachilo, S. M.; Strano, M. S.; Kittrell, C.; Hauge, R. H.; Smalley, R. E.; Weisman, R. B. *Science* **2002**, *298*, 2361.
- (11) Huang, S.; Dai, L. *J. Phys. Chem. B* **2002**, *106*, 3543.

JA048680J